AFRL-RV-PS-
TP-2015-0010

SHORT-PERIOD, ANELASTIC AND ANISOTROPIC, WAVEFORM-BASED 3D MIDDLE EAST MODEL TO IMPROVE NUCLEAR EXPLOSION MONITORING
Annual Report

Brian Savage, et al.

University of Rhode Island
317 Woodward Hall
9 East Alumni Ave
Kingston, RI 02881

30 August 2014

Technical Report

APPROVED FOR PUBLIC RELEASE; DISTRIBUTION IS UNLIMITED.

AIR FORCE RESEARCH LABORATORY
Space Vehicles Directorate
3550 Aberdeen Ave SE
AIR FORCE MATERIEL COMMAND
KIRTLAND AIR FORCE BASE, NM 87117-5776

DTIC COPY

NOTICE AND SIGNATURE PAGE

Using Government drawings, specifications, or other data included in this document for any purpose other than Government procurement does not in any way obligate the U.S. Government. The fact that the Government formulated or supplied the drawings, specifications, or other data does not license the holder or any other person or corporation; or convey any rights or permission to manufacture, use, or sell any patented invention that may relate to them.

This report was cleared for public release by the 377 ABW Public Affairs Office and is available to the general public, including foreign nationals. Copies may be obtained from the Defense Technical Information Center (DTIC) (http://www.dtic.mil).

AFRL-RV-PS-TP-2015-0010 HAS BEEN REVIEWED AND IS APPROVED FOR PUBLICATION IN ACCORDANCE WITH ASSIGNED DISTRIBUTION STATEMENT.

//SIGNED//	//SIGNED//
Dr. Robert Raistrick	Glenn M. Vaughan, Colonel, USAF
Project Manager, AFRL/RVBYE	Chief, Battlespace Environment Division

This report is published in the interest of scientific and technical information exchange, and its publication does not constitute the Government's approval or disapproval of its ideas or findings.

REPORT DOCUMENTATION PAGE

Form Approved
OMB No. 0704-0188

Public reporting burden for this collection of information is estimated to average 1 hour per response, including the time for reviewing instructions, searching existing data sources, gathering and maintaining the data needed, and completing and reviewing this collection of information. Send comments regarding this burden estimate or any other aspect of this collection of information, including suggestions for reducing this burden to Department of Defense, Washington Headquarters Services, Directorate for Information Operations and Reports (0704-0188), 1215 Jefferson Davis Highway, Suite 1204, Arlington, VA 22202-4302. Respondents should be aware that notwithstanding any other provision of law, no person shall be subject to any penalty for failing to comply with a collection of information if it does not display a currently valid OMB control number. **PLEASE DO NOT RETURN YOUR FORM TO THE ABOVE ADDRESS.**

1. REPORT DATE *(DD-MM-YYYY)*	**2. REPORT TYPE**	**3. DATES COVERED** *(From - To)*
30-08-2014	Technical Report	25 June 2013 – 24 June 2014

4. TITLE AND SUBTITLE
SHORT-PERIOD, ANELASTIC AND ANISOTROPIC, WAVEFORM-BASED 3D MIDDLE EAST MODEL TO IMPROVE NUCLEAR EXPLOSION MONITORING
Annual Report

5a. CONTRACT NUMBER
FA9453-12-C-0208

5b. GRANT NUMBER

5c. PROGRAM ELEMENT NUMBER
62601F

6. AUTHOR(S)
Brian Savage, Christina Morency, Brian M. Covellone, Arthur Rodgers, and Jeroen Tromp

5d. PROJECT NUMBER
1010

5e. TASK NUMBER
PPM00013629

5f. WORK UNIT NUMBER
EF007740

7. PERFORMING ORGANIZATION NAME(S) AND ADDRESS(ES)
University of Rhode Island
317 Woodward Hall
9 East Alumni Ave
Kingston, RI 02881

8. PERFORMING ORGANIZATION REPORT NUMBER

9. SPONSORING / MONITORING AGENCY NAME(S) AND ADDRESS(ES)
Air Force Research Laboratory
Space Vehicles Directorate
3550 Aberdeen Avenue SE
Kirtland AFB, NM 87117-5776

10. SPONSOR/MONITOR'S ACRONYM(S)
AFRL/RVBYE

11. SPONSOR/MONITOR'S REPORT NUMBER(S)
AFRL-RV-PS-TP-2015-0010

12. DISTRIBUTION / AVAILABILITY STATEMENT
Approved for public release; distribution is unlimited. (377ABW-2015-0339 dtd 04 May 2015)

13. SUPPLEMENTARY NOTES

14. ABSTRACT

Initial work improving the seismic waveform predictive capabilities for the Middle East adjoint tomography model demonstrated that enhancements were possible up to 15 seconds. These results at longer periods are in agreement with previous studies of the region. Full waveforms and adjoint techniques were used to identify deficiencies in the wave speed model. Initially, to progress to a minimum period of 15 seconds, transverse isotropy with a vertical symmetry axis was used in the mantle to stabilize the inversion. Travel times of all types of seismic waves showed the largest variance reduction, whereas there was minimal improvement of amplitude variations. Moreover, use of 3D wave speed models in source studies showed a dramatic improvement in the percent double couple of moment tensors over the entire data set.

Future work will continue to improve the seismic waveform predictive capability of the Middle East adjoint tomography model. We intend to reduce the minimum period as much as possible allowing for use of shorter period arrivals, smaller sized sources, and data with smaller signal to noise ratios. To reach shorter periods, the 3D anelastic attenuation variations will become increasingly important and will be incorporated into the Middle East model. At shorter periods, knowledge of the 3D anelastic attenuation structure will improve the fit to the amplitudes. Incorporation of 3D anisotropy will also be essential as the minimum period continues to decrease. We will relax the current constraint of a vertical symmetry axis for transverse isotropy in an attempt to recover the anisotropy in the Asian continental lithosphere and surrounding microplates.

Improved methods for routinely computing seismic waveforms at shorter periods will require larger computational and clustered systems, and improved, highly optimized algorithms and routines to reduce unnecessary computation.

15. SUBJECT TERMS
Adjoint method, Attenuation, Anisotropy, waveforms, 3D

16. SECURITY CLASSIFICATION OF:			**17. LIMITATION OF ABSTRACT**	**18. NUMBER OF PAGES**	**19a. NAME OF RESPONSIBLE PERSON**
a. REPORT	**b. ABSTRACT**	**c. THIS PAGE**			Dr. Robert Raistrick
Unclassified	Unclassified	Unclassified	Unlimited	20	**19b. TELEPHONE NUMBER** *(include area code)*

This page is intentionally left blank.

Approved for public release; distribution is unlimited.

Table of Contents

Approved for public release; distribution is unlimited.

Figures

Approved for public release; distribution is unlimited.

1. SUMMARY

Utilization of the full, seismic-waveform based techniques for discrimination purposes is currently effective and efficient for large magnitude, > M 4.5, well-recorded events. However, a need to reduce the magnitude threshold requires predictive capabilities at shorter periods, <~10 seconds, if waveform based techniques are to be used in routine event evaluations. Recent efforts to improve the seismic waveform, prediction capabilities of existing models have proven successful by reducing an acceptable period for prediction to 15 - 20 seconds. As models begin to accurately predict shorter periods, they will begin to incorporate higher order structures, i.e. larger and sharper wave speed contrasts, and they will also be effective in source discrimination at shorter periods and high noise environments. However, as the minimum period continues to drop, effects of attenuation and anisotropy will become more significant and require quantification. As such, current generation models lack both heterogeneous anelastic attenuation and a more robust treatment of anisotropy. We plan on pushing the predictive capabilities of the current 3D Middle East wave speed model to shorter periods. In doing so, 3D anleastic attenuation and anisotropic models will be incorporated into a seamless seismic Earth model of the Middle East region. Anelastic attenuation will be embedded along side a 3D wave speed model and the anisotropic component will be parameterized as transverse isotropy with a variably oriented symmetry axis.

Achieving these ambitious goals requires a waveform based, tomographic inversion capable of handling seismic waveform propagation, 3D variations in attenuation, and general anisotropy. As with previous efforts use of the SPECFEM3D Globe and its adjoint tomographic capabilities will perform the necessary forward and time-reversed calculations. Demands required by the short period requires use of large clustered computer systems and improved / state-of-the-art computational units to efficiently simulate the seismic wavefield. An initial step of source characterization demonstrated that this is invaluable to accurately predict waveform amplitudes with minimal change to the source moment tensor, but only at stations near amplitude nodes. Predicting wave-field amplitudes are increasingly important, as anelastic attenuation is highly dependent on variations in seismic amplitudes. Initial inversions for seismic wave speeds began at longer periods and later inversions incorporated additional shorter period energy. Our results show wave speed anomalies began to localize and strengthen in amplitude; similar effects for attenuation and anisotropy are also expected. The final model, with a enhanced predictive capabilities, 3D anelastic attenuation, and anisotropy with a variably oriented symmetry axis will be a major advance for the Nuclear Explosion Monitoring community for event discriminate at smaller magnitudes.

2. INTRODUCTION

This work aims to improve predictions of full-waveform seismic signals from regional events within the Middle East region. When complete, responses from events within the study region will be characterized and predicted at shorter periods. Previous results utilizing only wave speeds, Vp, Vsv and Vsh, were able to adequately reproduce recorded events down to 15

Approved for public release; distribution is unlimited.

seconds. Updates to the 3D wave speed model significantly reduced travel time misfit but did not improve differences in amplitude. Further enhancements will require the incorporation of 3D attenuation and more complex treatment of anisotropy. Iterative improvements to the 3D Earth model, including wave speed, attenuation and anisotropy, are accomplished through an adjoint method that identifies regions of the model that require improvement. The adjoint method incorporates the physics of wave propagation and finite-frequency effects and can improve predictions of travel times and amplitudes, i.e. the full waveform.

Improvement of the 3D Earth model will radically enhance source discrimination investigations. Significant limitations to full-waveform source studies are the lack of Earth models that accurately predict the path-specific Green's functions. While these source investigations are quite robust at discriminating between a variety of source types (e.g. Liu et al, 2004; Minson and Dreger, 2008; Ford et al., 2009; Kim et al., 2011), the limited predictive capabilities of wave speed models restrict their periods use to greater than 30 – 50 seconds. Use of these long periods necessitates sources to be a minimum magnitude, nominally > 4.5 Mw. Efforts to enhance the waveform predictive capabilities of wave speed models have recently begun to shift the minimum period to ~15 seconds at regional distances. The recent and future improvement of these full waveform predictive models will allow the investigation of sources at even lower magnitudes, ~ 3.0 Mw, dependent on epicentral distance.

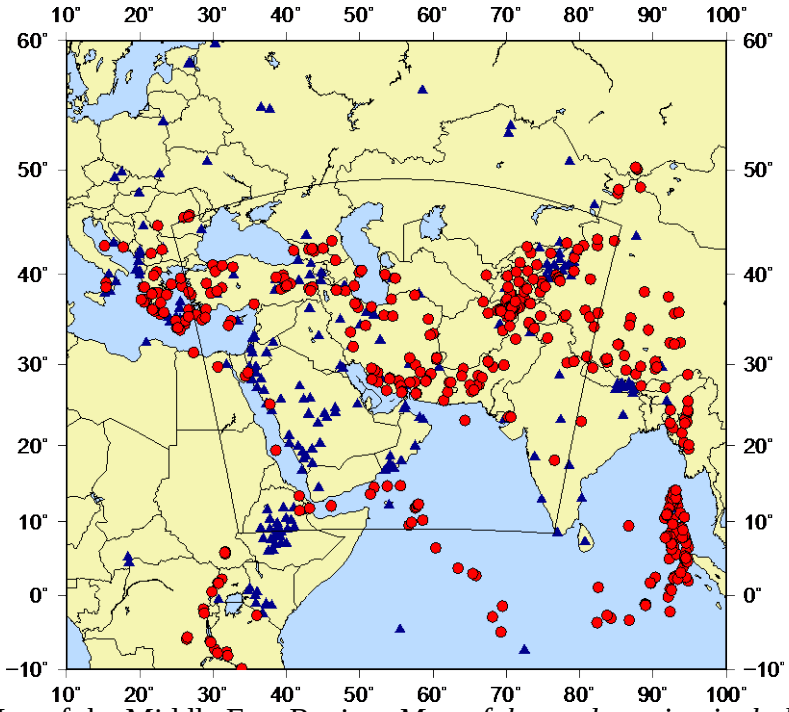

Figure 1. Map of the Middle East Region. *Map of the study region including events as red circles and stations as blue triangles. The original mesh, black outline, was approximately 45 degrees on a side and easily capable of computing synthetics to a minimum period of 11 seconds. A new expanded mesh is 90 degrees on a side and includes the many more events and stations not included in the original mesh design.*

Approved for public release; distribution is unlimited.

3. TECHNICAL APPROACH

3.1. Earth Model Tomography

Extending the predictive period range of the Middle East model will be undertaken using the adjoint capabilities of SPECFEM3D_GLOBE. Essential to the adjoint tomographic method (Tromp et al., 2005) and improving 3D Earth models is the ability to calculate the regular and adjoint wavefields in an existing 3D Earth model. The regular wavefield, or forward field, is defined as the displacement at all points for all times from a traditional seismic source. While the adjoint wavefield is defined as the displacement at all points for all reversed times from adjoint waveform sources. The adjoint waveform source is a user-defined measure between the true response at a seismic station, the data, and the predicted response, the synthetic. This measure can be a simple difference between the data and synthetics, a least squares differences, a metric isolating travel time or amplitude differences, or any combination. For this specific project, we use a multi-taper methodology to measure frequency-dependent delays in travel time and differences in amplitude. A summation of the regular and adjoint fields over time generates Frechét derivatives that isolate deficiencies in the current model, i.e., where the model requires improvement. The adjoint method implemented here sums the regular and adjoint fields during back-propagation, or while the forward field runs backwards in time. This summation eliminates the requirement of storing the regular and adjoint fields for all times.

Adjoint techniques use full seismic wave propagation physics and incorporate finite-frequency wave propagation effects. These methods have been used with impressive results in the Middle East (Savage et al., 2011, 2012, 2014), Southern California (Tape et al., 2009), and Europe (Zhu et al., 2013). Many of the current advanced seismic tomographic techniques include various fundamentals of the adjoint methodology, but do not exploit the full waveform to improve the predictive response of surface and body waves in tandem. A simple example of creating the kernels is displayed in Figure 2 with a single source and single receiver.

This new adjoint tomography experiment will increase the seismic data by ~30% through the inclusion of more recent seismic events (Figure 1). The data set will also vastly increase due to the ability to model smaller magnitude events at shorter periods. Event and station distributions (Figure 1) have not changed much from the initial experiment, but regions of interest tectonically have instrumentally expanded thus adding more seismic data.

Efforts to extend the period range to even shorter periods require higher resolution images of wave speeds, plus incorporation of increasingly important effects of anelastic attenuation, Q^{-1}, and anisotropy. With decreasing period these second-order effects, at long period <30 seconds, become important and can radically alter seismic paths and recorded responses. The goal of this effort is to further improve models of seismic wave speeds, Vs and Vp, to predict seismic waveforms at periods approaching 2 seconds. In addition, anelastic attenuation and anisotropy will also be accounted for through improved use of amplitude anomalies and parameterization.

Approved for public release; distribution is unlimited.

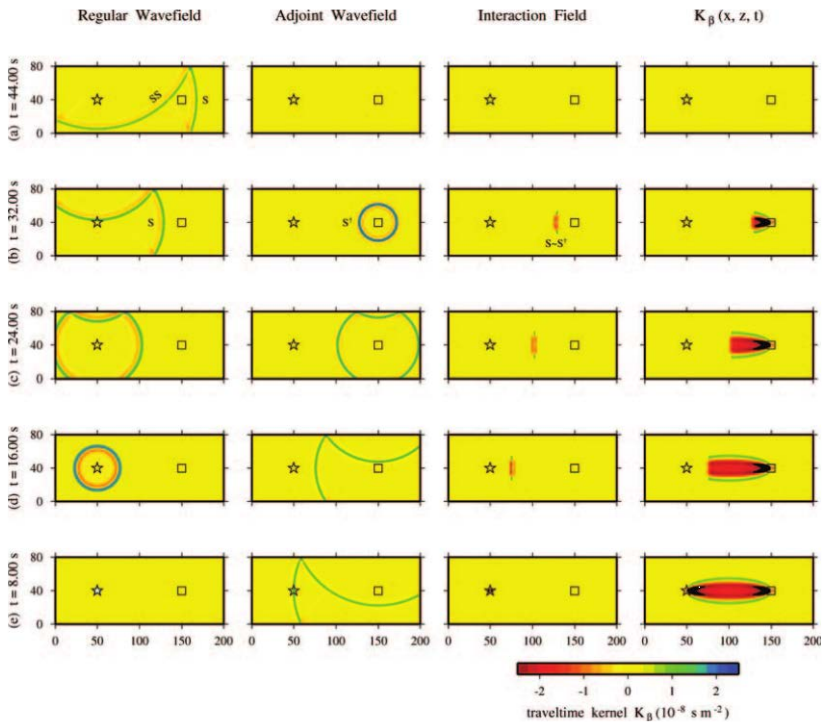

Figure 2. Example of adjoint kernel creation. *Example of the adjoint tomography method, where time increases in each row starting from the bottom, the first two columns are the regular and adjoint wavefields, the third column is the interaction, or multiplication, between the first two columns and the fourth column is the kernel, or time summation/integration of the third column. Notice the regular wavefield propagates from the source, star, to the receiver, box, in forward time (bottom row to top row) and the adjoint field propagates from the receiver to the station, but in reverse time (top row to bottom row). From Tromp et al. (2005)*

3.2. Source Re-evaluations

In addition to improvement to the Earth model, seismic sources are reevaluated in an effort to reduce artifacts. Source related artifacts in the final model are a result of errors in the fault plane solution and hypocenter. We use a straightforward moment tensor inversion outlined in Liu et al. (2004) to account for and eliminate these errors. The advantage of the methodology is the flexibility to use synthetic seismograms from any methodology, including the improved 3D Earth model. We solve for the best fitting moment tensor solution and depth, constrained by a zero-trace solution. Moreover, we also solve for the best fitting double couple, full moment tensor, and perform an error analysis. In practice, all moment tensor solutions are quite similar to the preferred solution and to the initial solution provided by either the Global CMT solution or previous work by Covellone and Savage (2012). Solution errors are normally quite small as defined by the spread of P- and T-axes, and improvements to the sources show up at azimuths close to nodal planes of the radiation pattern. Recorded responses show rapid changes in amplitudes around nodal planes, thus small changes in the source solution can dramatically alter

Approved for public release; distribution is unlimited.

a the response for a near nodal station. With these minor changes, we anticipate a further increase in the double couple component for all events as the model continues to improve.

The inversion requires synthetics from initial solution, obtained from Global CMT or Covellone and Savage (2012), a perturbed depth source, and sources for each of the six moment tensor elements. Each of these sources is computed using the current iteration model, M14, thus requiring 8 simulations per source and a short hiatus of the tomography iterations. However, once the simulations are complete, source inversions are very fast and exploited during a bootstrap, error analysis.

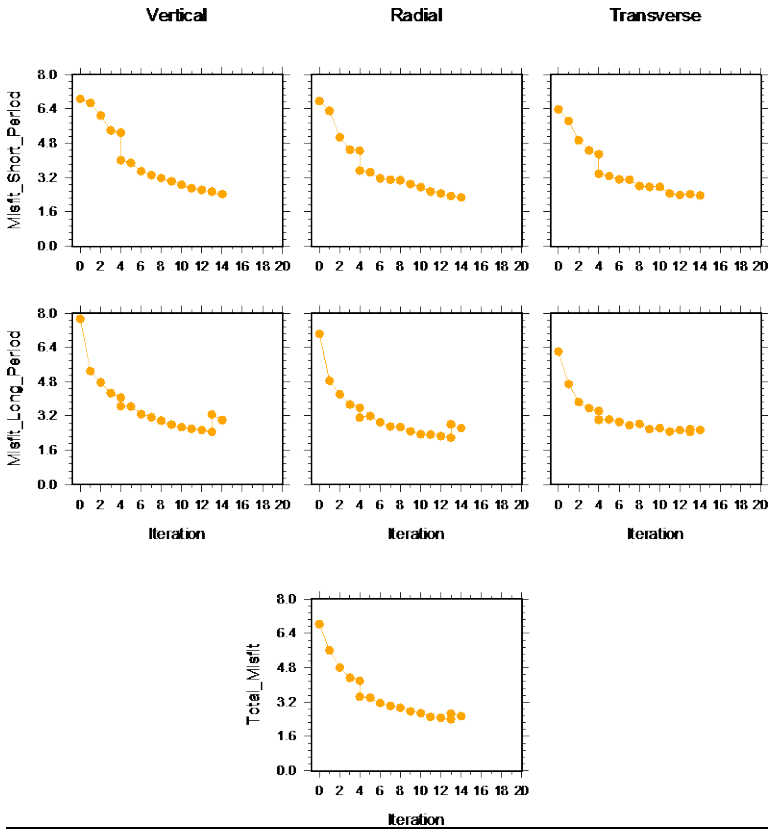

Figure 3. Misfit between data and synthetics against iteration. *Total misfit (bottom) is separated into individual components (columns in first and second rows) and into short (top row) and long period (middle row) bands. The short period band involves primarily body waves, while the long period band is for surface waves. A step in the misfit at iteration 4 is due to a change in both period bands.*

4. RESULTS AND DISCUSSION

Adjoint tomographic inversions were completed up to iteration 14 and include transverse isotropy with a vertical symmetry axis using measurements of phase delay. Using the flexible measurement tool FLEXWIN (Maggi et al. 2009), measurements of misfit were easily made for surface and body waves simultaneously on three components and in two different period bands. The misfit for all components and the total misfit are displayed in Figure 3.

Approved for public release; distribution is unlimited.

During each iteration, improvements to the model are made and the misfit is reduced for all components and all period bands. The most significant improvements are during the initial iterations, but as the iterations progresses the misfit and the improvements to the model are reduced and the misfit plateaus, both are expected behaviors. A significant step in the misfit at iteration 4 is due to a modification of the period bands for both long and short periods. The long period was expanded from a range of 40-120 seconds to 30-120 seconds, but the short period was reduced from 14-40 seconds to 14-30 seconds. The reduction in the short period band accounts for most of the drop in misfit at this iteration. A second change to the parameterization was made at iteration 7 where the lateral smoothing was reduced from 100 km to 50 km, but this appears to have little impact on the overall improvement of the model.

At iteration 14, the period ranges are currently 14-30 seconds and 20-120 seconds. Iteration 14 also represents the transition to a larger computational and model domain that includes many more events, stations and usable data than in previous iteration, Figure 4. In the new model, for regions outside of the original model domain the initial wave speed model, M00, was used while model iteration 13, M13, was used within. This expansion of the model does not significantly alter the total misfit between M13 and M14. The increase in events, stations, and ray-based path coverage is displayed in Figure 4. Expanding the model domain introduces stations in northern Asia, eastern Europe, and in the Indian Ocean along with a vast number of events in Tibet and post-2007 events. The path coverage represents usable data with measurement windows as determined by FLEXWIN.

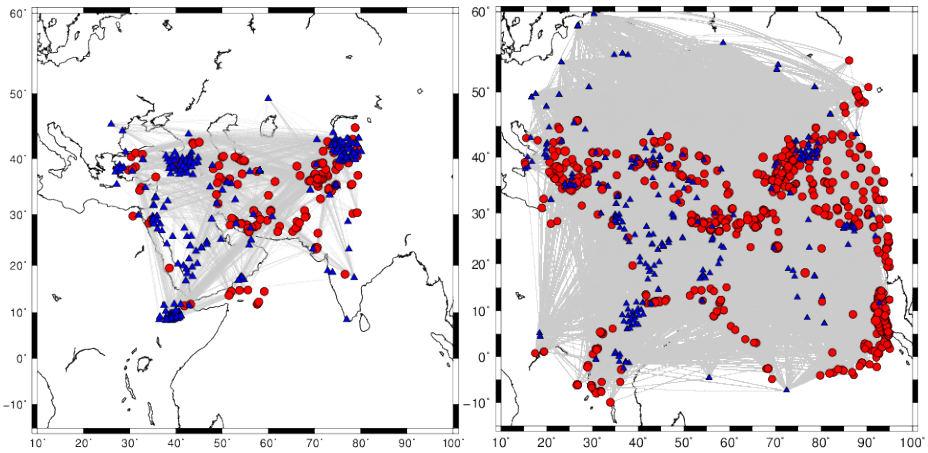

Figure 4. Comparison of path coverage between old and new models. *Ray path coverage in the original model domain (left) and the new, larger model domain (right). The original model domain contained 182 events and 356 stations, but not all the stations had workable signals. The new model domain includes 468 events and 241 stations, all with usable signals.*

The current model for the Middle East, M14, is displayed in Figure 5 as absolute wave speed and a wave speed perturbation. The wave speed perturbation indicates a total change of around 6% in vertical shear wave speed, Vsv from the initial 3D model, M00, S2.9EA (Kustowski et al., 2008). A number of well known, large-scale tectonic features appear within the model further suggesting that the inversion is converging on a true representation of the Earth. Beneath the Persian Gulf, there is a subducted Neo-Thethys oceanic lithosphere, faster than average, trending

Approved for public release; distribution is unlimited.

to the northeast and extending throughout much of the upper mantle. Low wave speeds in the central and southern Red Sea extending into the Gulf of Aden are quite significant down to at least 200 km depth. Finally, subducting Indian lithosphere is identified beneath the western most edge of Tibet as well as thickened crust not accounted for in the initial model appears as a reduction in wave speed at shallow depths, < 75km.

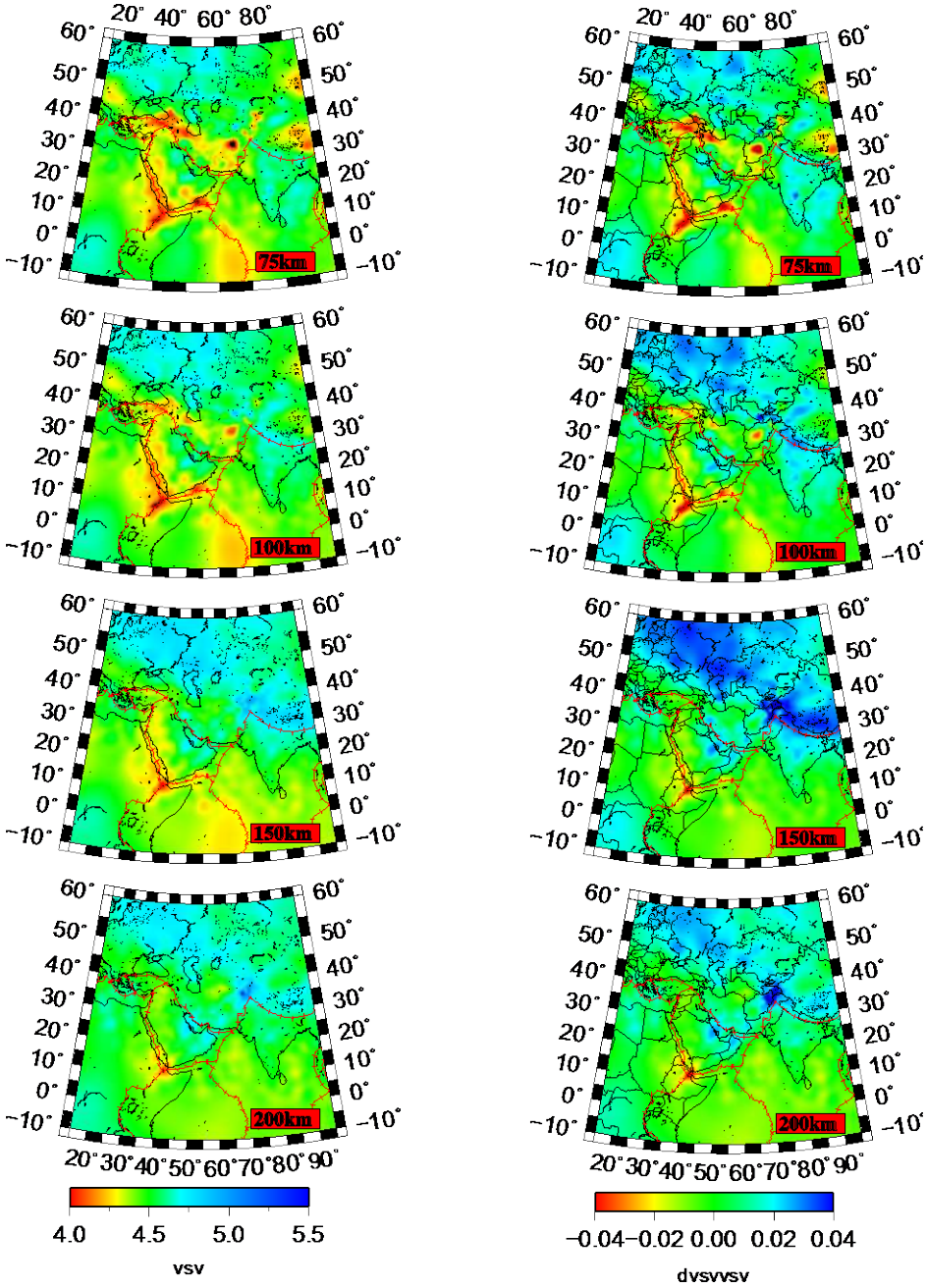

Figure 5. Current iteration wave speed model of the Middle East. *Absolute vertical shear wave speed, Vsv, is shown in the left column and wave speed perturbation of Vsv is in shown the right column plotted at depths of 75, 100, 150 and 200 km.*

Approved for public release; distribution is unlimited.

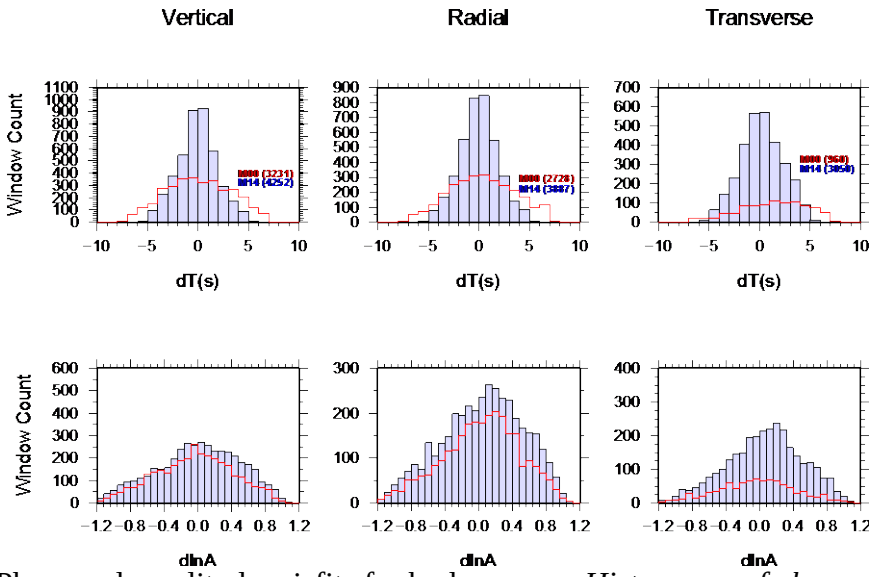

Figure 6. Phase and amplitude misfits for body waves. *Histograms of phase, dT, and amplitude, dlnA, mismatch from the initial model, M00, and the current model. The initial model is the single line in red and the current model is the filled light blue bars. Improvement to both the phase and amplitude are apparent across all components. Phases are body waves measured between 14 and 30 seconds period.*

Improvement in the predictive capabilities of the current iteration model is demonstrated in Figures 6 and 7. For the short period band, primarily body waves, the phase and amplitude mismatch is shown for the initial model, M00, and the current model, M14. For a perfect fit, phase and amplitude mismatch should be 0.0. Phase measurements for all three components show a vast improvement from the initial to the current model. The phase misfit distribution is narrower with a larger peak around zero, indicating a larger portion of body wave arrivals are matched with zero-lag time. Results are similar for the longer period band that highlights surface wave arrivals.

Amplitude misfits are also reduced while only measurements of phase delay are used to improve the model. Improvements to amplitude data are not as significant as those for phase delay, but this is expected. The combination of the minimal improvement to the amplitude measurements and the misfit at later iterations suggests that amplitude measurements should be included in the inversion in an effort to update the attenuation structure. This initially will increase the misfit due to the added measurements, but we should obtain a robust, combined wave speed and attenuation model. We plan on starting iterations including attenuation during the initial stages of the upcoming year.

An example of improvements to the model and its predictive capabilities for an individual event-station path is shown in Figure 8. A synthetic response on the western side of the model from an event near the western syntaxis of Tibet demonstrates improvements to the model. For all three components there is a significant improvement in the fit to the data. Surface waves, both Rayleigh and Love, show good travel time agreement using the current model as opposed to large time shifts seen from responses from the initial model. Higher frequency body waves,

Approved for public release; distribution is unlimited.

particularly on the radial component at 712 seconds, show improved agreement with the data in the updated model. These radial S wave arrivals appear quite poorly matched when using the initial model, in amplitude and phase. Response of the current model for these arrivals shows a dramatic improvement in phase but at the expense of increased amplitude. This might indicate a need for greater attenuation along these paths. As shown by the histograms in Figures 6 and 7, many of the synthetic responses show improvement in a similar manner as demonstrated for the single event-station path in Figure 8.

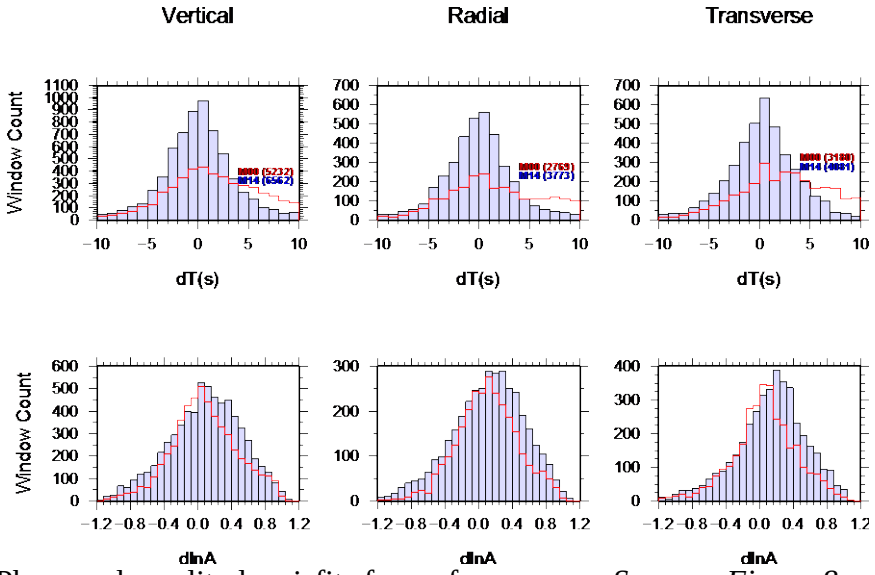

Figure 7. Phase and amplitude misfits for surface waves. *Same as Figure 8 except for surface waves measured between 24 and 120 seconds period.*

Due to the reduced misfit vs. iteration for the last few iterations and the less than optimal fit of waveform amplitudes, demonstrated by the raw waveforms and the amplitude misfit for the entire data set, upcoming iterations of the Middle East model will use the expanded model shown in Figures 1 and 4. This modification of the inversion parameters will reduce the overall misfit, but is required as further iterations using the current parameters and data sets are not able to account for the variance identified in the data (see the amplitude mismatch in the waveforms displayed in Figure 8). New major changes will be 1) an introduction of amplitude measurements and the ability to solve for a 3D attenuation model, 2) the relaxing of constraints on anisotropy by solving for the symmetry axis orientation along with Vsv and Vsh, and 3) the introduction of a vastly larger data set and model domain. The addition of a 3D attenuation model and amplitude measurements have successfully been implemented in a European model, building on prior work by Zhu et al. (2013). Relaxing the anisotropy constraints will improve fits to surface wave arrivals for continental paths with complex tectonic histories.

Approved for public release; distribution is unlimited.

5. CONCLUSIONS

Initial work improving the seismic waveform predictive capabilities for the Middle East adjoint tomography model demonstrated that enhancements were possible up to 15 seconds. These results at longer period are in agreement with previous studies of the region. Full waveforms and adjoint techniques were used to identify deficiencies in the wave speed model. Initially, to progress to a minimum period of 15 seconds, transverse isotropy with a vertical symmetry axis was used in the mantle to stabilize the inversion. Travel times of all types of seismic waves showed the largest variance reduction, whereas there was minimal improvement of amplitude variations. Moreover, use of 3D wave speed models in source studies showed a dramatic improvement in the percent double couple of moment tensors over the entire data set.

Future work will continue to improve the seismic waveform predictive capability of the Middle East adjoint tomography model. We intend to reduce the minimum period as much as possible allowing for use of shorter period arrivals, smaller sized sources, and data with smaller signal to noise ratios. To reach shorter periods, the 3D anelastic attenuation variations will become increasingly important and will be incorporated into the Middle East model. At shorter periods, knowledge of the 3D anelastic attenuation structure will improve the fit to the amplitudes. Incorporation of 3D anisotropy will also be essential as the minimum period continues to decrease. We will relax the current constraint of a vertical symmetry axis for transverse isotropy in an attempt to recover the anisotropy in the Asian continental lithosphere and surrounding microplates.

Improved methods for routinely computing seismic waveforms at shorter periods will require larger computational and clustered systems, and improved, highly optimized algorithms and routines to reduce unnecessary computation.

Approved for public release; distribution is unlimited.

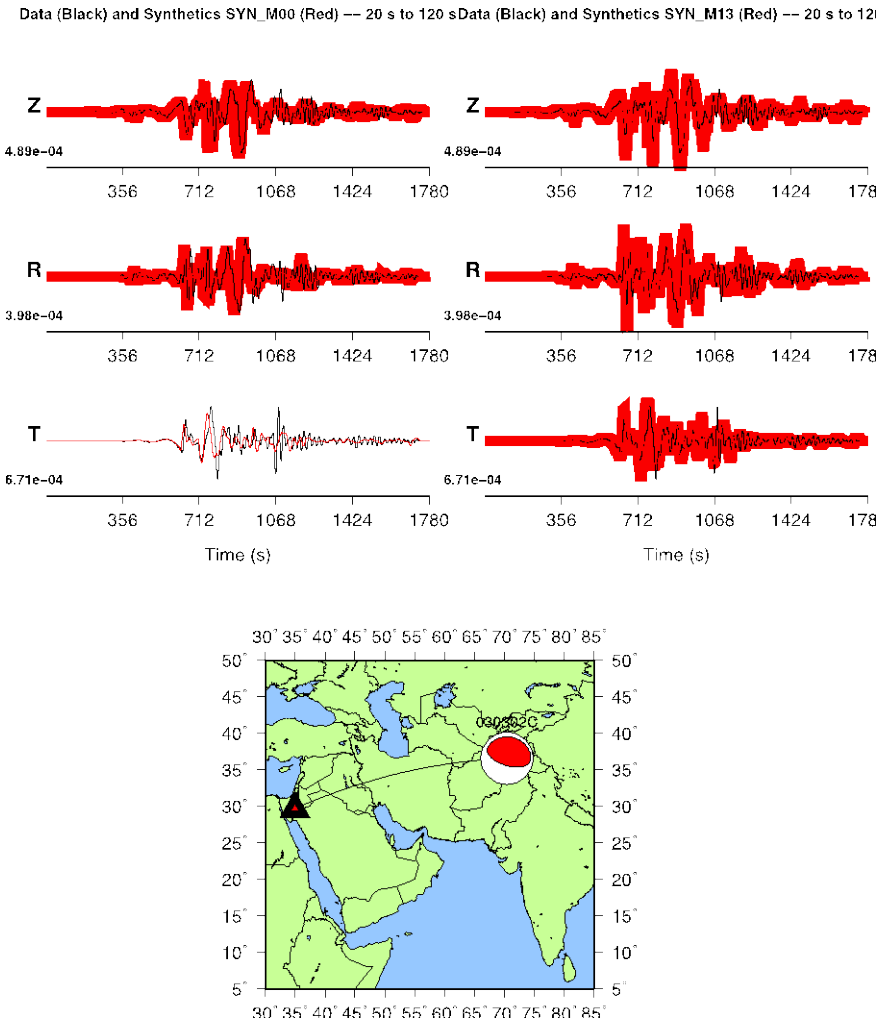

Figure 8. Comparison of waveforms fits for a single event-station path. *Single station-event response difference between the initial model, left, and the current model, right. Data is shown in black and synthetic responses are in red. All three components, vertical, radial and tangential are display at 20 to 120 seconds. The improvement to the model aligns the synthetic response with the data, primarily the surface waves.*

Approved for public release; distribution is unlimited.

REFERENCES

Covellone, B. M. and B. Savage (2012), A Quantitative Comparison Between 1D and 3D Source Inversion Methodologies: Application to the Middle East, Bull. Seism. Soc. Am., 102 (5).

Ford, S., D. Dreger, and W. Walter (2009), Source analysis of the Memorial Day explosion, Kimchaek, North Korea, Geophysical Research Letters, 36(21), L21, 304.

Kim, Y., Q. Liu, and J. Tromp (2011), Adjoint Centroid-Moment Tensor inversions, Geophys. J. Int. 186, pp. 264-278. doi: 10.1111/j.1365-246X.2011.05027.x.

Kustowski, B., G. Ekstrom, and A. Dziewonski (2008), The shear-wave velocity structure in the upper mantle beneath eurasia, Geophys, J. Int., 174, pp. 978-992, doi:10.1111/j.1365-246X.2008.03865.x.

Liu, Q., J. Polet, D. Komatitsch, and J. Tromp (2004), Spectral-Element Moment Tensor Inversions for Earthquakes in Southern California, Bull. Seism. Soc. Am., 94(5), pp. 1748-1761, doi:10.1785/012004038.

Maggi, A., C. Tape, M. Chen, D. Chao, and J. Tromp (2009), An Automated time-window selection algorithm for seismic tomography, Geophys. J. Int., 178(1), pp. 257-281, doi:10.1111/j.1365-246X.2009.04099.x.

Minson, S. and D. Dreger (2008), Stable inversions for complete moment tensors, Geophysical Journal International, 174(2), pp. 585-592.

Savage, B., D. B. Peter, B. M. Covellone, A. J. Rodgers, and J. Tromp (2011), Next generation, waveform based three-dimensional models and metrics to improve nuclear explosion monitoring in the Middle East, in Proceedings: 33th Monitoring Research Review (MRR 2011).

Savage, B., D. Peter, B. M. Covellone, A. J. Rodgers, and J. Tromp (2012), Next Generation, Waveform based 3-Dimensional Models and Metrics to Improve Nuclear Explosion Monitoring in the Middle East, Final Report AF8718-09-C-0009, Air Force Research Laboratory, Hanscom AFB, MA.

Savage, B., C. Morency, B. M. Covellone, A. Rodgers, and J. Tromp (2014), Short-period, anelastic and anisotropic, waveform-based 3D Middle East model to improve nuclear explosion monitoring, Review of Monitoring Reserach, New Mexico, June 17-19, 2014.

Tape, C., Q. Liu, A. Maggi, and J. Tromp (2009), Adjoint tomography of the Southern California crust, Science, 325, pp. 988-992, doi: 10.1126/science.1175298.

Tromp, J., C. Tape, and Q. Liu (2005), Seismic tomography, adjoint methods, time reversal and banana-doughnut kernels, Geophysical Journal International, 160 (1), pp. 195-216.

Zhu, H., E. Bozdag, T. S. Duffy, and J. Tromp (2013), Seismic attenuation beneath Europe and the North Atlantic: implications for water in the mantle, Earth and Planetary Science Letters, 381, pp. 1-11.

DISTRIBUTION LIST

DTIC/OCP
8725 John J. Kingman Rd, Suite 0944
Ft Belvoir, VA 22060-6218 1 cy

AFRL/RVIL
Kirtland AFB, NM 87117-5776 2 cys

Official Record Copy
AFRL/RVBYE/Dr. Robert Raistrick 1 cy

Approved for public release; distribution is unlimited.

This page is intentionally left blank.

Approved for public release; distribution is unlimited.